Local SAR Control for Parallel Transmit MRI using Multiple Patient Models

Hanno Homann[1], Inagmar Graesslin[1], Ulrich Katscher[1], Peter Vernickel[1], Kay Nehrke[1], and Peter Börnert[1]
[1]*Philips Research Laboratories, Hamburg, Germany*

Introduction Parallel transmission enables control of the RF transmit field in space and time. Hence, not only the B_1 field but also the distribution of the specific absorption rate (SAR) within the patient body can be influenced [1,2]. A reduction of the body-averaged and local SAR is highly desirable, since this parameter often limits scan performance in high-field MRI. As the local SAR is difficult to measure, numerical simulations are required to predict the local SAR [3]. This is, however, challenging since the local SAR does not only depend on the multi-channel drive, but also shows considerable patient dependency. In this study, patient-specific SAR models and a generalized SAR model are considered for SAR control in a whole body parallel transmit MR system.

Methods Finite-Difference Time-Domain (FDTD) simulations were performed using a model of a 3T body coil with eight independent transmit elements [4]. Dielectric human body models were generated from nine volunteers, based on water-fat-separated whole-body scans as described in [5]. This discrimination between water-rich and fatty tissues was found to be relevant for accurate SAR prediction [5]. All volunteer models were placed inside the model of the Tx body coil and RF simulations were carried out for each Tx element separately.

Based on the simulated E and B_1 field sensitivities ($\mathbf{S}_E$ and $\mathbf{S}_{B1}$), SAR calculations (Eqs. 1,2) and RF shimming (Eq. 3) were performed. Here, $\mathbf{w}$ denotes the vector of complex channel weights and $\mathbf{Q}(\mathbf{r})$ is an 8x8 matrix for each voxel in the body model, containing pre-computed local averages over 10g for fast SAR calculation [6].

First, RF shimming was carried out without additional constraints. For a more targeted local SAR management, RF shimming was then repeated with local SAR constraints (Eq. 4) [7]. For optimization, the SAR constraints were incorporated into the magnitude least-squares cost function [8] by the barrier method [9]. As it is computationally not efficient to consider every voxel $\mathbf{r}$ in a body model, a model compression technique [10] was applied to ignore those voxels where the maximum local SAR cannot occur (for a given additive uncertainty margin). SAR-constrained RF-shimming was performed using (a) the volunteer-specific SAR models and (b) using a generalized SAR model, which was obtained by combining the Q-matrices of all volunteer models, and applying the model compression technique a second time [11].

$$\mathrm{SAR}(\mathbf{r}) = \mathbf{w}^H \cdot \underbrace{\frac{1}{V}\int_V \frac{\sigma}{2\rho}\mathbf{S}_E^H(\mathbf{r})\mathbf{S}_E(\mathbf{r})\mathrm{d}V}_{\mathbf{Q}(r)} \cdot \mathbf{w} \quad (1)$$

$$= \mathbf{w}^H \mathbf{Q}(\mathbf{r})\mathbf{w} \quad (2)$$

$$||\,|\mathbf{S}_{B1}\cdot\mathbf{w}| - \mathbf{B}_{1,target}||_2^2 \;\rightarrow\; \min \quad (3)$$

$$s.t. \quad \mathbf{w}^H\cdot\mathbf{Q}(\mathbf{r})\cdot\mathbf{w} \;\leq\; \mathrm{SAR}_{\max} \quad (4)$$

Results With RF shimming, the RF field homogeneity was significantly improved in all cases (coefficient of variation CV=11.0%-16.6%) compared to quadrature excitation (CV=23.7%-37.5%). Furthermore, the SAR distribution inside the body was often found to be more homogeneous (cf. Fig. 1). RF shimming generally led to a substantial reduction of the local SAR even without SAR constraints for all volunteers (SAR reduction by 28.6%-52.0% and 24.4%-82.8% in the torso and the arms, respectively).

A further SAR reduction could be obtained in the SAR-constrained optimization (reduction by 51.3%-77.4% and 53.5%-75.2% in the torso and the arms, respectively) using the selected SAR limits (SAR_{max} = 10W/kg and 20W/kg in the torso and the arms, respectively) while maintaining high B_1 performance (CV=11.6%-20.4%). The SAR-constrained algorithm converged within a few seconds and showed only linear time-dependence on the number voxels in the (compressed) body model. Using the generalized model, the SAR limits were still maintained for all models with only a marginal increase in computation time, but at slightly decreased B_1 homogeneity (CV=13.0%-22.6%).

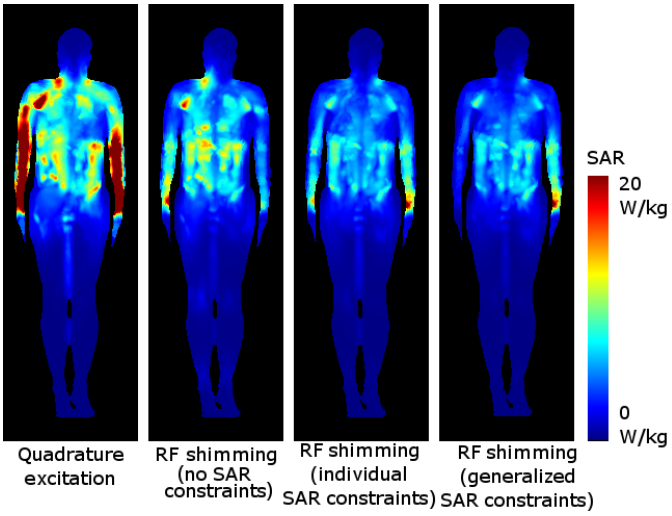

Fig. 1: Maximum intensity projections of the predicted 10g SAR simulated for one of the volunteer models for different RF excitations (normalized to B_1 = 2μT).

Discussion and Conclusions RF shimming was observed to result in lower SAR, which is probably a consequence of the spatially more homogeneous B_1 distribution (according to Ampere's law). Using the volunteer-specific SAR constraints, a further SAR reduction could be achieved. In a clinical setting, such models are however typically not available. Instead, a generalized model representing a multitude of patient anatomies and body positions inside the RF coil could be applied. In this study, it was demonstrated that such a generalized approach does not necessarily entail increased computation times or severe compromises in B_1 performance.

Overall, the freedom in the MR sequence design can certainly be increased by RF shimming with simultaneous control of the local SAR. Considering multiple body models is important for robust SAR prediction. Local SAR control can be achieved with reasonable computational effort in real time.

References [1] C.v.d.Berg, MRM;57:577-586 (2007) [2] D.Brunner, MRM;63:1280-1291 (2010) [3] C.Collins, MRM;65:1470-1482 (2011) [4] P.Vernickel, MRM;58:381-389 (2007) [5] H.Homann, MRM, DOI:10.1002/ mrm.22948 (2011) [6] I.Graesslin, Proc. ISMRM, p.74 (2008) [7] H.Homann, MAGMA (2011) [8] Setsompop, MRM;59:908-915 (2008) [9] S.Boyd, Convex Optimization, Cambridge University Press (2004) [10] M.Gebhardt, Proc. ISMRM, p.1441 (2010) [11] H.Homann, Proc. ISMRM, p.3843 (2011)